

# A Comparative Study of Iron Uptake Mechanisms in Marine Microalgae: Iron Binding at the Cell Surface Is a Critical Step<sup>1[W][OA]</sup>

Robert Sutak, Hugo Botbol, Pierre-Louis Blaiseau, Thibaut Léger, François-Yves Bouget, Jean-Michel Camadro, and Emmanuel Lesuisse\*

Department of Parasitology, Faculty of Science, Charles University, 12844 Prague, Czech Republic (R.S.); Université Pierre et Marie Curie (Paris 06), Centre National de la Recherche Scientifique Unité Mixte de Recherche 7621, Laboratoire d'Océanographie Microbienne, F-66651 Banyuls/Mer, France (H.B., F.-Y.B.); and Université Paris Diderot (Paris 07), Centre National de la Recherche Scientifique, Institut Jacques Monod, F-75013 Paris, France (P.-L.B., T.L., J.-M.C., E.L.)

We investigated iron uptake mechanisms in five marine microalgae from different ecologically important phyla: the diatoms *Phaeodactylum tricornerutum* and *Thalassiosira pseudonana*, the prasinophyceae *Ostreococcus tauri* and *Micromonas pusilla*, and the coccolithophore *Emiliania huxleyi*. Among these species, only the two diatoms were clearly able to reduce iron, via an inducible (*P. tricornerutum*) or constitutive (*T. pseudonana*) ferrereductase system displaying characteristics similar to the yeast (*Saccharomyces cerevisiae*) flavohemoproteins. Iron uptake mechanisms probably involve very different components according to the species, but the species we studied shared common features. Regardless of the presence and/or induction of a ferrereductase system, all the species were able to take up both ferric and ferrous iron, and iron reduction was not a prerequisite for uptake. Iron uptake decreased with increasing the affinity constants of iron-ligand complexes and with increasing ligand-iron ratios. Therefore, at least one step of the iron uptake mechanism involves a thermodynamically controlled process. Another step escapes to simple thermodynamic rules and involves specific and strong binding of ferric as well as ferrous iron at the cell surface before uptake of iron. Binding was paradoxically increased in iron-rich conditions, whereas uptake per se was induced in all species only after prolonged iron deprivation. We sought cell proteins loaded with iron following iron uptake. One such protein in *O. tauri* may be ferritin, and in *P. tricornerutum*, Isip1 may be involved. We conclude that the species we studied have uptake systems for both ferric and ferrous iron, both involving specific iron binding at the cell surface.

There are two main strategies for iron uptake by terrestrial microorganisms and plants, and both have been characterized in the yeast *Saccharomyces cerevisiae* (for review, see Kosman, 2003; Philpott and Protchenko, 2008; Blaiseau et al., 2010). The first is the reductive mechanism of uptake. Extracellular ferric complexes are dissociated by reduction via transplasma membrane electron transfer catalyzed by specialized flavohemoproteins (Fre). In

yeast, free ferrous iron is then imported as such, or by a high-affinity permease system (Ftr) coupled to a copper-dependent oxidase (Fet), allowing iron to be channeled through the plasma membrane (this reoxidation step is not found in higher plants). In the second strategy, the siderophore-mediated mechanism, siderophores excreted by the cells or produced by other bacterial or fungal species are taken up without prior dissociation via specific, copper-independent high-affinity receptors. The iron is then dissociated from the siderophores inside the cells, probably by reduction (for review, see Philpott, 2006; Blaiseau et al., 2010). *Chlamydomonas reinhardtii* is a model photosynthetic eukaryotic freshwater organism for the study of iron homeostasis and shares with yeast the first strategy of iron uptake (iron reduction followed by uptake involving reoxidation of iron by a multicopper oxidase; Merchant et al., 2006; Allen et al., 2007).

Much less is known about the strategies used by marine phytoplankton to acquire iron. There is evidence that these two strategies are used by some marine microalgae (for review, see Morrissey and Bowler, 2012). A yeast-like reductive uptake system has been suggested in the marine diatoms *Thalassiosira pseudonana* (Armbrust et al., 2004) and *Phaeodactylum tricornerutum* (Kustka et al., 2007; Allen et al., 2008; Bowler et al., 2008) on the basis of gene

<sup>1</sup> This work was supported by the French Agence Nationale de la Recherche (grant no. ANR 11 BSV7 018 02 "PhytoIron"), by the Ministry of Education of the Czech Republic (grant no. MSM 0021620858), by a Marie Curie European Reintegration Grant (within the 7th European Community Framework Program) project no. UNCE 204017, and by the Centre National de la Recherche Scientifique (Centre National de la Recherche Scientifique fellowship to H.B.).

\* Corresponding author; e-mail lesuisse.emmanuel@ijm.univ-paris-diderot.fr.

The author responsible for distribution of materials integral to the findings presented in this article in accordance with the policy described in the Instructions for Authors ([www.plantphysiol.org](http://www.plantphysiol.org)) is: Emmanuel Lesuisse (lesuisse.emmanuel@ijm.univ-paris-diderot.fr).

<sup>[W]</sup> The online version of this article contains Web-only data.

<sup>[OA]</sup> Open Access articles can be viewed online without a subscription.

[www.plantphysiol.org/cgi/doi/10.1104/pp.112.204156](http://www.plantphysiol.org/cgi/doi/10.1104/pp.112.204156)

sequence homology and transcriptomic analyses, and copper-dependent reductive uptake of iron has been demonstrated for *Thalassiosira oceanica* (Maldonado et al., 2006). The existence of marine siderophores has also been established (Butler, 1998, 2005; Mawji et al., 2008), and their use by certain microalgae as an iron source, through reductive or nonreductive mechanisms, has been documented (Soria-Dengg and Horstmann, 1995; Naito et al., 2008; Hopkinson and Morel, 2009). However, for most marine unicellular eukaryotes, the mechanisms of iron assimilation are completely unknown. The strategies used by these organisms to acquire iron must have evolved to adapt to the very particular conditions that prevail in their surrounding natural environment: the transition metal composition of the ocean differs greatly from that of terrestrial environments (Butler, 1998). The form in which iron exists in ocean water remains unclear. Morel et al. (2008) suggested that unchelated iron may be an important source of iron for phytoplankton, whereas other authors have suggested that most of the ferric iron in ocean water is complexed to organic ligands, with conditional stability constants in the range of  $10^{11}$  to  $10^{22} \text{ M}^{-1}$  (Rue and Bruland, 1995; Butler, 1998). Colloidal iron has been identified as a major form of iron at the surface of the ocean (Wu et al., 2001). In any case, iron levels in surface seawater are extremely low (0.02–1 nM; Turner et al., 2001). Most existing research supports the general model of iron uptake by marine eukaryotic phytoplankton, involving membrane transporters that directly access dissolved monomeric inorganic iron species (Sunda, 2001): in *T. pseudonana*, for example, iron uptake is related to the concentration of unchelated ferric iron species ( $\text{Fe}'$ ) and is independent of the concentration of iron chelated to synthetic ligands (Sunda, 2001; Morel et al., 2008). We found that this also applies to *Chromera velia* (Sutak et al., 2010). Depending on the ligands present in the system, the equilibrium free ferric ion ( $\text{Fe}'$ ) concentration is in the range of  $10^{-16}$  to  $10^{-19} \text{ M}$ , a concentration that seems incompatible with the functioning of any classic metal transport system. No classic iron uptake system with a  $K_d$  in the nanomolar range has ever been found. A strategy of iron uptake operating efficiently in a terrestrial environment that contains iron at micromolar concentrations may thus be ineffective in a marine environment. Additionally, the marine environment imposes physical limits on the classic strategies of uptake, including the high diffusion rate of the species of interest, notably siderophores and reduced iron (Völker and Wolf-Gladrow, 1999). Therefore, there are likely to be completely different mechanisms of iron uptake in phytoplanktonic algae that have not yet been discovered. Photoreductive dissociation of natural ferric chelates or ferric colloids in seawater could increase the “free” iron ( $\text{Fe}'$ ) concentration available for transport by over 100-fold (Sunda, 2001). Consequently, dark/light cycles may be relevant to the regulation of these postulated iron uptake systems in phytoplanktonic species.

The fate of intracellular iron in marine microalgae is also poorly understood. As in all plants, iron is primarily

involved in the electron transfers required for photosynthesis and respiration, but little is known about how phytoplanktonic species adapt to iron scarcity. In chronically low-iron regions, the lack of iron in seawater, and the resulting decrease in iron uptake, could theoretically trigger two kinds of metabolic responses in addition to the changes observed in cell morphology (Allen et al., 2008; Marchetti et al., 2009). The cells may mobilize intracellular iron stores, if present, or adapt their metabolism to reduce the requirement for iron for electron transfer and energy production. Intracellular iron stores, in the form of ferritin, have only been evidenced in pennate diatoms (Marchetti et al., 2009), although ferritin genes have now been detected in several species (Allen et al., 2008; Monnier et al., 2010). Different kinds of metabolic responses of eukaryotic phytoplankton to iron starvation have also been proposed, mainly on the basis of whole-genome analyses (Finazzi et al., 2010), but very few experimental data are available, and when available, the authors generally used ferric EDTA as the only iron source. Ferric EDTA is widely used as the iron source for studies of iron uptake by marine microalgae (Anderson and Morel, 1982; Shaked et al., 2005; Shaked and Lis, 2012), because EDTA buffers an easily calculated pool of unchelated iron ( $\text{Fe}'$ ) in the medium (Shaked et al., 2005). However, the stability constants ( $\log K_f$ ) of ferric and ferrous EDTA are both very high (25.7 and 14.3, respectively); thus, using ferric EDTA as an iron source in experiments of iron uptake does not allow discrimination between reductive and nonreductive uptake. Most ferric ligands, unlike EDTA, have a much lower stability constant for ferrous iron than for ferric iron, and this is the reason why the reductive iron uptake system is so powerful: it catalyzes the dissociation of ferric iron from most of its ligands by reduction, allowing ferrous iron to be taken up by a unique system from very different ferric chelates. The estimated stability constant for the monoiron(III) dicitrate complex is in the range ( $\log$ ) 19.1 to 38.7 (Silva et al., 2009), and for the ferrous complex it is about ( $\log$ ) 3. This explains how yeast cells can take up ferric citrate and different ferri-siderophore complexes reductively, but not ferric EDTA (Lesuisse and Labbe, 1989). Intermediates of the Krebs's cycle have been shown to be good candidates for iron ligation in seawater (Vukosav and Mlakar, 2010). We thus used ferric citrate as the main source of ferric iron and ferrous ascorbate as the main source of ferrous iron (the iron sources generally used in the yeast model), although we also studied other iron sources but in less detail.

We tried to determine experimentally the main features of iron uptake from these iron sources by five phylogenetically unrelated microalgae species representative of the marine and oceanic eukaryotic phytoplankton. We chose species that have their genomes sequenced and that are living in different ecological niches. Among the picoplanktonic prasinophytes, we studied the widespread coastal species *Ostreococcus tauri*, the smallest eukaryotic organism described until

now, and *Micromonas pusilla*, which is the dominant photosynthetic picoeukaryote in the western English Channel (Not et al., 2004). Among the important group of diatoms, we studied the centric diatom *T. pseudonana* and the pennate diatom *Phaeodactylum tricornutum*, because genomic studies on both species allowed the identification of genes putatively involved in iron metabolism and in the response to iron starvation (Armbrust et al., 2004; Allen et al., 2008). Finally, the oceanic species *Emiliania huxleyi* was chosen for this study, as it is the most abundant coccolithophore found in the Earth's oceans. The position of each species on a eukaryotic phylogenetic tree (Cepicka et al., 2010) is shown in Figure 1.

Our main goal was to identify the strategies of iron uptake (reductive or nonreductive) in these different species and the differences between them. We also examined the conditions, if any, of induction of the mechanisms of iron uptake.

## RESULTS

### Iron Requirement and Storage

We compared the iron requirements of the selected species by growing each of them with a series of concentrations of ferric citrate or in the presence of the hydroxamate siderophores ferrioxamine B (FOB) or ferrichrome (FCH), with a 100-fold excess of the desferri-siderophores desferrichrome and desferriferrioxamine B (DFOB) to ensure that all of the iron medium was complexed by the siderophores (Supplemental Table S1). We evaluated their ability to accumulate and store iron when added as ferric citrate (0.1 or 1  $\mu\text{M}$ ) to the growth medium (Table I). The five species showed nearly maximum growth rate (in exponential growth phase)

with iron concentration as low as 0.01  $\mu\text{M}$  in the medium, although this iron concentration was limiting for biomass production, except for *E. huxleyi* (Supplemental Fig. S1). This is indicative of very-high-affinity iron uptake systems and of high iron requirements. The diatom *T. pseudonana* showed the highest iron requirement, both in terms of maximum growth rate in the exponential growth phase and of biomass production: this species grew nearly 2-fold faster in the exponential phase (first 3 d of culture) and produced 4.5-fold more cells in the stationary phase (after 10 d of culture) when the iron concentration in the medium was shifted from 1 nM to 1  $\mu\text{M}$  (Supplemental Table S1). In contrast, even the lowest iron concentration tested (1 nM) did not slow the growth of the coccolithophore *E. huxleyi*, and maximum biomass production (cell yield) by this species was reached at 0.01  $\mu\text{M}$  (Supplemental Table S1). Iron concentrations of 1  $\mu\text{M}$  or higher were toxic (as assessed from the growth rate; data not shown) for *E. huxleyi*. The growth rate of *T. pseudonana* continued to increase with increasing iron concentration up to 10  $\mu\text{M}$  (the highest concentration we tested; data not shown). Thus, these two species have very different physiological responses to changes in the concentration of iron in the medium. The other species tested showed intermediate iron requirements in the order *O. tauri* > *M. pusilla* > *P. tricornutum* (Supplemental Table S1). The green algae *O. tauri* and *M. pusilla* showed generally similar behavior in terms of iron requirement and storage: the effects of iron concentration on the growth rate and biomass yield were very similar (Supplemental Table S1), and both species accumulated nearly identical amounts of iron (Table I).

Addition of the hydroxamate siderophore FCH or FOB (0.01  $\mu\text{M}$ ) with a large excess of the corresponding desferriferri-siderophores (1  $\mu\text{M}$ ) strongly or completely inhibited the growth of *O. tauri*, *M. pusilla*, and *T. pseudonana* but inhibited the growth of *E. huxleyi* and *P. tricornutum* more weakly, as reported previously (Soria-Dengg and Horstmann, 1995; Supplemental Table S1). Thus, two of the species were able to use iron initially bound to hydroxamate siderophores for growth (see below).

All the species were able to accumulate iron from the medium very efficiently (Table I). For comparison, yeast cells show optimum growth rate and cell yield when the concentration of iron in the medium is about 10  $\mu\text{M}$ , leading to an intracellular concentration of iron of about 100 to 200  $\mu\text{M}$  (Seguin et al., 2010). Clearly, the enrichment factor (cell-associated versus extracellular iron) was much higher in all the microalgae species tested, indicating the expression of very efficient mechanisms of iron uptake and concentration, as already described (for review, see Morrissey and Bowler, 2012). The two species of diatom overaccumulated iron more than the other species in the presence of excess iron (1  $\mu\text{M}$ ): a 10-fold increase in the concentration of iron in the medium led to a nearly 10-fold increase of iron associated with *T. pseudonana* cells (Table I). *T. pseudonana* cells in stationary phase (with a mean volume of 100  $\mu\text{m}^3$  per cell)

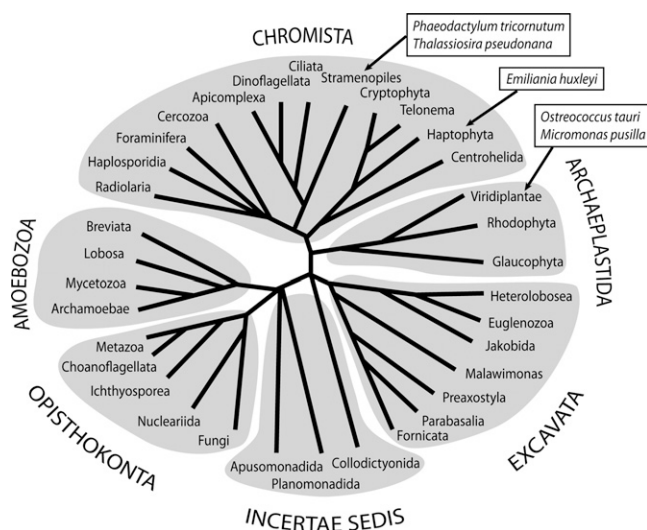


**Figure 1.** Eukaryotic phylogenetic tree showing the positions of the five marine microalgae species selected in this work.

**Table 1.** Iron associated with the cells as a function of the iron concentration in the medium

Cells were grown with either 0.1 or 1  $\mu\text{M}$  ferric citrate, harvested in the stationary phase, and washed with strong iron chelators as described in "Materials and Methods." Iron associated with the cells was then determined. Values are expressed in pmol iron 1 million cells<sup>-1</sup> and in  $\mu\text{M}$  iron within the cells (values in parentheses). Values shown are means  $\pm$  SD from three experiments.

Species	Fe 0.1 $\mu\text{M}$	Fe 1 $\mu\text{M}$
<i>P. tricornutum</i>	10.2 $\pm$ 0.8 (65)	52.3 $\pm$ 12.3 (350)
<i>T. pseudonana</i>	5.99 $\pm$ 0.54 (50)	53.56 $\pm$ 6.48 (450)
<i>O. tauri</i>	0.59 $\pm$ 0.12 (400)	0.99 $\pm$ 0.07 (670)
<i>M. pusilla</i>	0.40 $\pm$ 0.02 (150)	1.02 $\pm$ 0.16 (390)
<i>E. huxleyi</i>	11.99 $\pm$ 0.72 (80)	34.54 $\pm$ 7.65 (240)

had accumulated about 70% of the total iron present in the culture medium (1  $\mu\text{M}$ ). In contrast, the smallest species, *O. tauri* (1  $\mu\text{M}$ <sup>3</sup>), increased its cellular iron content by only about 1.6-fold when the iron concentration was increased from 0.1 to 1  $\mu\text{M}$  and accumulated about 10% of the iron present in the medium at this latter concentration (Supplemental Tables S1 and S2). In all species, the amount of iron accumulated by the cells clearly exceeded the cellular iron requirements, which implies the existence of iron storage mechanisms. These preliminary experiments show that the patterns of iron acquisition and accumulation differ between phylogenetically unrelated marine microalgae, suggesting different mechanisms of iron uptake and responses to iron starvation and iron excess.

## General Methodology

We investigated whether the uptake of ferric and/or ferrous ions and/or iron chelates could be induced/repressed by growth conditions. We also tested whether the species studied used a reductive mechanism of iron uptake, involving the expression of an inducible or a constitutive ferrireductase activity. The cells were precultured in either low-iron modified f (Mf) medium (0.01  $\mu\text{M}$ ) or in high-iron Mf medium (1  $\mu\text{M}$ ) for 1 week, harvested, and washed. The cells were then distributed equally into fresh high-iron Mf medium (2  $\mu\text{M}$ ) and into fresh iron-deficient Mf medium (no iron added). Cells were harvested from samples of these new cultures every day for 10 to 15 d and examined for ferrireductase and iron uptake activities. When cells reached late exponential or stationary phase, they were diluted in the same iron-rich and iron-deficient media. An example of the growth curves and ferrireductase activities obtained in one such experiment is shown in Figure 2.

## Cell Ferrireductase Activity and Transplasma Membrane Electron Transfer

*P. tricornutum* exhibited a ferrireductase activity that was induced after prolonged iron starvation (Fig. 1), whereas *T. pseudonana* showed constitutive ferrireductase

activity (Fig. 2). The activity of this ferrireductase was in the same order of magnitude as that of the Frel-dependent ferrireductase in iron-deficient yeast cells (0.5–2 nmol h<sup>-1</sup> 1 million cells<sup>-1</sup>). Transcriptomic analyses, comparative genomic studies, and direct measurements of reductase activity have indicated the presence of a reductive system of iron uptake in diatoms (Shaked et al., 2005; Maldonado et al., 2006; Allen et al., 2008). Here, we show that the ferrireductase activity is regulated by iron availability in one diatom and constitutively expressed in another. In *P. tricornutum*, induction of ferrireductase activity was rapid but delayed by 7 d after the shift from high-iron medium to iron-deficient medium (Fig. 2). This lag period was decreased to 3 d when the cells were precultured in low-iron medium (0.01  $\mu\text{M}$ ) and shifted to iron-deficient medium (data not shown).

The green algae *M. pusilla* and *O. tauri* exhibited very low or undetectable ferrireductase activity (Fig. 2): in *M. pusilla*, the ferrireductase activity was iron independent and at least 1,000-fold weaker than that in diatoms; and in *O. tauri* and *E. huxleyi*, no ferrireductase activity was detected under any growth conditions (Fig. 2). Note that the sensitivity of the colorimetric assay we used may be too low to evidence very weak, but possibly significant, reductase activity. We previously showed that the transplasma membrane electron transport involved in the reduction of extracellular ferric complexes by yeast cells could be measured with a highly sensitive fluorometric assay based on reduction of the nonpermeant (blue) resazurin dye (electron acceptor) to resorufin (fluorescent red; Lesuisse et al., 1996). The inducible yeast reductase activity (using either resazurin or Fe<sup>3+</sup> as electron acceptor) is strongly inhibited by diphenylene iodonium (DPI), a powerful inhibitor of the neutrophil

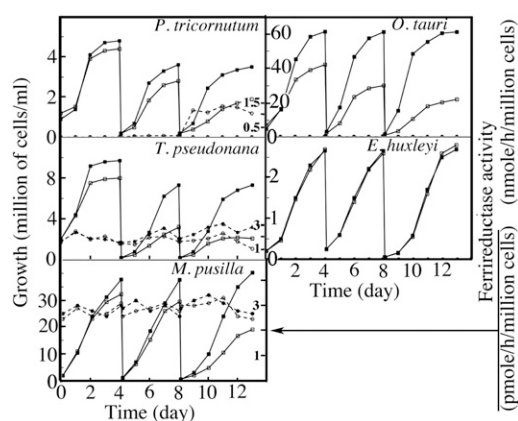


**Figure 2.** Iron-dependent growth and ferrireductase activity of the five marine microalgae species selected in this work. The cells were precultured in iron-rich medium (1  $\mu\text{M}$ ) for 1 week and washed, and aliquots were shifted to iron-rich medium (closed symbols) and iron-deficient medium (open symbols). Growth (squares) and ferrireductase activity (circles) were determined daily. When the cells reached the end of the exponential growth phase, they were diluted in the same medium. Data are from one representative experiment.

NADPH oxidase (Doussi re and Vignais, 1992) and more generally of flavohemoproteins (Lesuisse et al., 1996). Therefore, we tested whether the algae species were able to reduce resazurin and measured the effect of DPI on resazurin reduction, using yeast cells as a reference (Fig. 3). The diatom species showed transplasma membrane electron transfer to resazurin, and this activity was inducible by iron deprivation in *P. tricornutum* and was constitutive in *T. pseudonana*, in agreement with the results of the colorimetric assay for iron reduction (Fig. 3). In both species, resazurin reduction was strongly inhibited by DPI, as in yeast, suggesting that flavohemoproteins (like Fre1 in yeast) are responsible for the ferrireductase activity in diatoms, as suggested previously (Allen et al., 2008; Morrissey and Bowler, 2012). Surprisingly, the green algae *M. pusilla* and *O. tauri* showed significant resazurin reductase activity (Supplemental Fig. S1), although ferrireductase activity in both species was very low or undetectable (Fig. 2). In these species, transplasma membrane electron transfer to resazurin was not induced by iron deprivation and was not inhibited by DPI (Supplemental Fig. S1). This suggests that the proteins involved in this activity are not related to the Fre family. *E. huxleyi* failed to reduce resazurin (Supplemental Fig. S1), consistent with findings for the alveolate *C. velia* (Sutak et al., 2010). Our results strongly support the hypothesis that diatoms can use a reductive mechanism for iron uptake, as suggested previously (Shaked et al., 2005; Allen et al., 2008).

### Kinetics of Iron Uptake from Ferric and Ferrous Iron Sources

We investigated iron uptake from the following iron sources: ferric citrate, ferrous ascorbate, ferric EDTA, and hydroxamate siderophores (FOB and FCH). We

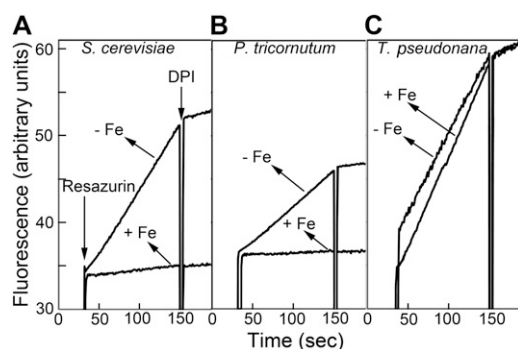


**Figure 3.** Reductase activity of yeast and diatoms with resazurin as the electron acceptor. A, Transplasma membrane electron transfer by whole cells was monitored by fluorimetric analysis of the formation of resorufin from resazurin (10  $\mu\text{M}$ ). Yeast was used as a control. Yeast cells were grown overnight in iron-rich (10  $\mu\text{M}$ ; +Fe) or iron-deficient (–Fe) medium. B and C, *P. tricornutum* (B) and *T. pseudonana* (C) were grown for 1 week in iron-rich (1  $\mu\text{M}$ ; +Fe) or iron-deficient (–Fe) medium. Yeast and diatoms were suspended at 100 million cells  $\text{mL}^{-1}$  in citrate/Glc buffer and in Mf medium, respectively, and the formation of resorufin was monitored. The inhibitor DPI was added to a final concentration of 10  $\mu\text{M}$  as indicated.

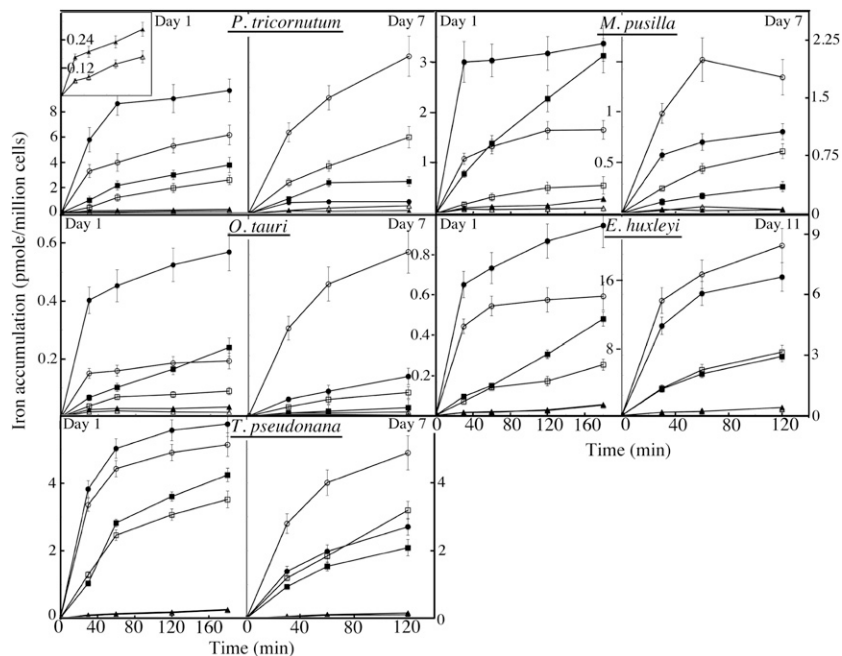
recorded the kinetics of iron uptake by cells harvested daily 6 h after the beginning of the light period in a night/day cycle of 8/16 h (for 10–15 d) from iron-rich and iron-deficient media (Fig. 2). Uptake kinetics were recorded either in the dark or in the light (3,000 lux). We will present selected representative results.

We did not observe major differences in short-term (2-h) iron uptake kinetics (from either ferric citrate or ferrous ascorbate) recorded in the dark or in the light (Supplemental Fig. S2). This suggests that photoreduction of ferric citrate was negligible under our experimental conditions, and most of the iron uptake kinetics were thus followed in the light.

Figure 4 shows typical kinetics of uptake from ferric citrate (1:20), ferric EDTA (1:1.2), and ferrous ascorbate (1:50) by the five selected species after 1 and 7 d (or 11 d for *E. huxleyi*) of growth in iron-rich and iron-deficient media (according to the pattern presented in Fig. 2). In all species, iron was taken up much more rapidly from ferric citrate than from ferric EDTA, and ferrous iron (ferrous ascorbate) was generally taken up more rapidly than ferric iron (ferric citrate). Both ferric and ferrous iron uptake activities were inducible by iron deprivation in all species, but there was a lag between shifting the cells from iron-rich to iron-deficient conditions and induction: this lag period was 3 d for *T. pseudonana*, 4 to 5 d for *O. tauri* and *M. pusilla*, 7 d for *P. tricornutum*, and 11 to 12 d for *E. huxleyi* (Fig. 4; data not shown). This lag could have been the consequence of iron bound to the cell surface when shifted, although the cells were washed with strong ferric and ferrous chelators before inoculation of the iron-deficient medium (see below). More surprisingly, species shifted from high-iron Mf medium (1  $\mu\text{M}$ ) to fresh high-iron Mf medium (2  $\mu\text{M}$ ) exhibited higher iron uptake activities (especially during the first 30–60 min of the kinetics) than cells shifted to iron-deficient medium (Fig. 4). A similar transient induction of iron uptake activities (which lasted for several days) occurred following a shift from low-iron medium (0.01  $\mu\text{M}$ ) to high-iron medium (2  $\mu\text{M}$ ; data not shown). This is suggestive of two different mechanisms of induction of iron uptake and/or binding, one responding rapidly to iron-rich conditions and the other responding after a prolonged period of iron deprivation.

Although some species were able to grow with hydroxamate siderophores as iron sources (Supplemental Table S1), the rate of iron uptake from FOB and FCH by all the species tested was similar to (for FCH) or slower than (for FOB) the rate of iron uptake from ferric EDTA and very much slower than that from ferric citrate (data not shown). Direct transport of hydroxamate siderophores mediated by specific receptors, therefore, is unlikely, although a gene encoding a putative FCH transporter has been found in *P. tricornutum* (Allen et al., 2008). Iron uptake from hydroxamate siderophores probably occurred either reductively (in diatoms) or after nonreductive dissociation of  $\text{Fe}^{3+}$  from its ligands (as is probably the case for iron uptake from ferric EDTA).

**Figure 4.** Iron uptake from various iron sources ( $1 \mu\text{M}$ ) by the five marine microalgae species selected in this work, harvested after 1, 7, or 11 d of growth in iron-rich (closed symbols) or iron-deficient (open symbols) medium. Squares represent ferric citrate (1:20), circles represent ferrous ascorbate (1:50), and triangles represent ferric EDTA (1:1.2). The insert in the top left panel shows iron uptake from ferric EDTA at a different y scale. Values shown are means  $\pm$  SD from four experiments.



In all species we tested, the rate of iron uptake from citrate, EDTA, or hydroxamate (siderophore) ferric complexes decreased substantially as the ligand-to- $\text{Fe}^{3+}$  ratio increased, as observed previously for the alveolate *C. velia* (Sutak et al., 2010) and for *Thalassiosira weissflogii* (Shaked et al., 2005). An example is shown in Figure 5 for ferric citrate. This observation strongly suggests that iron uptake is dissociative in all five species studied (i.e. that iron must be dissociated from its ligands prior to uptake by the cells). This observation also suggests that at least one limiting step of iron uptake is controlled thermodynamically rather than kinetically and does not involve a mechanism of iron channeling through the membrane, unlike what is observed in the high-affinity reductive iron uptake system of yeast (Kwok et al., 2006).

#### Iron Reduction Is Not a Prerequisite for Iron Uptake

The results presented above and previous observations (Shaked et al., 2005; Allen et al., 2008; Morrissey and Bowler, 2012) suggest that some phytoplanktonic algae use a reductive mechanism for iron uptake. This is particularly evident for the diatom *P. tricornutum*, because both iron uptake and ferrireductase activity were induced by iron deprivation in this species. However, all of the species we studied were able to take up both ferric and ferrous iron, although ferrous iron was the preferred substrate in terms of uptake rate, regardless of the ferrireductase activity of the cells. For example, *P. tricornutum* acquired iron from ferric chelates even when its ferrireductase system was completely repressed (compare Figs. 2 and 4). Therefore, iron reduction may not be essential for iron uptake, unlike the situation in yeast. To evaluate the contribution of iron reduction to iron uptake from a ferric iron source, we measured the

effect of a large excess (200  $\mu\text{M}$ ) of the strong ferrous chelator bathophenanthroline disulfonic acid (BPS) on initial iron uptake rates from ferric citrate ( $1 \mu\text{M}$ ). The experiments were done in the dark to avoid photoreduction of ferric citrate, which is strongly promoted by BPS addition. After 15 min, BPS inhibited iron uptake

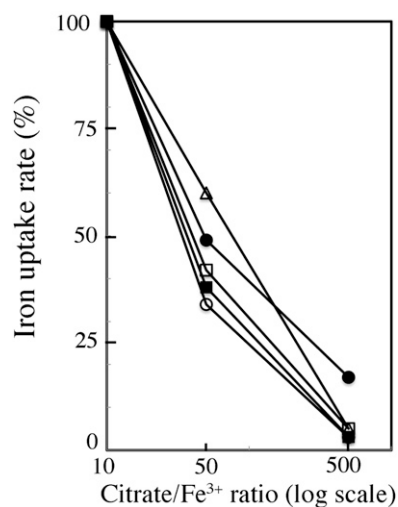


**Figure 5.** Effect of increasing the ligand (citrate)- $\text{Fe}^{3+}$  ratio on iron uptake. The cells (grown under standard conditions) were incubated for 1 h in uptake buffer with  $1 \mu\text{M}$   $\text{Fe}^{3+}$  complexed with 10, 50, or 500  $\mu\text{M}$  citrate, and iron taken up by the cells was determined. Results are expressed as percentage of the maximal uptake rate for each species. Open circles represent *P. tricornutum*, closed circles represent *T. pseudonana*, open squares represent *O. tauri*, closed squares represent *M. pusilla*, and triangles represent *E. huxleyi*. Values shown are means from four experiments. Error bars are not shown for the sake of clarity, but SD values in all cases were 7% or less.

by  $71\% \pm 3\%$  in *P. tricornutum*,  $78\% \pm 6\%$  in *T. pseudonana*,  $61\% \pm 3\%$  in *O. tauri*,  $65\% \pm 8\%$  in *M. pusilla*, and  $15\% \pm 2\%$  in *E. huxleyi* (mean  $\pm$  SD from three experiments; cells were cultured for 1 week in Mf medium without iron to induce iron uptake systems before uptake experiments). In yeast, for which iron reduction is a prerequisite for uptake, inhibition of ferric citrate uptake ( $1 \mu\text{M}$ ) by BPS ( $200 \mu\text{M}$ ) was  $95\% \pm 2\%$ , as shown previously (Sutak et al., 2010). The inhibitory effect of BPS on ferric citrate uptake was weakest for *E. huxleyi*, the only species studied to have no system for transplasma membrane electron transfer. Therefore, this species must have a nonreductive uptake system for ferric iron, as described previously for *C. velia* (Sutak et al., 2010). The inhibitory effect of BPS was highest for *P. tricornutum* and *T. pseudonana*, consistent with the rapid reduction of iron by these species, which can then be trapped by BPS. However, even in these species, BPS did not inhibit ferric citrate uptake as strongly as it does in yeast ( $95\%$ ). This difference could be due to ferrous iron being less available to BPS in marine microalgae than yeast suspensions for some unknown reason. However, it is more likely that all the algae species we studied are able to take up both ferric and ferrous iron, maybe via independent transporters.

#### Evidence That There Is an Iron-Binding Step at the Cell Surface Prior to Uptake

We used pulse-chase experiments to study the kinetics of iron uptake. Cells were grown for 1 week in standard conditions (Mf medium with  $0.1 \mu\text{M}$  iron), in high-iron conditions (Mf medium with  $1 \mu\text{M}$  iron), or in low-iron conditions (Mf medium with  $2 \text{ nM}$  iron). The yeast *S. cerevisiae* was used as a control. They were then incubated in the presence of  $^{55}\text{Fe}$  (ferric citrate or ferrous ascorbate) for 15 min, and a 10- to 100-fold excess of cold ferric or ferrous iron (in the same chemical form) was added (Figs. 6 and 7). As expected, uptake of  $^{55}\text{Fe}$  by yeast stopped (or substantially decreased) immediately upon addition of excess cold iron (Fig. 6), indicating that iron uptake occurs directly from iron in solution, without any intermediate step. Iron uptake by *T. pseudonana* from  $^{55}\text{Fe(III)}$ -citrate continued after the addition of a large excess of cold Fe(III)-citrate (Figs. 6 and 7). Similarly labeled ferrous iron uptake by *P. tricornutum* grown in low-iron medium continued after the chase (Fig. 7). Similar findings have been reported for *Pleurochrysis carterae* (Hudson and Morel, 1990), and the authors concluded that iron was taken up from the surface of the cells without reentering solution (Hudson and Morel, 1990). This appears to be the case for the species we analyzed: according to the redox state of iron, to the algae species, and to the growth conditions, addition of excess cold iron after that of  $^{55}\text{Fe}$  resulted in either an increase or a decrease of  $^{55}\text{Fe}$  associated with the cells, but never in complete arrest of  $^{55}\text{Fe}$  uptake, as would be expected for simple isotopic dilution (Figs. 6 and 7). As a control experiment, we tested the addition

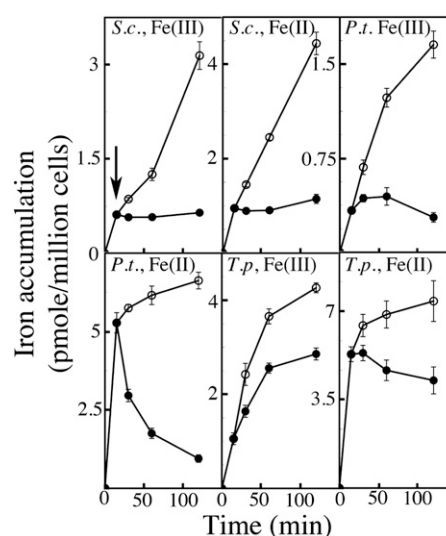


**Figure 6.** Pulse-chase uptake of iron (1). Yeast (*S.c.*), *P. tricornutum* (*P.t.*), and *T. pseudonana* (*T.p.*) cells (grown in Mf medium containing  $0.1 \mu\text{M}$  iron) were incubated in citrate/Glc buffer (yeast) or uptake buffer (microalgae) with either  $1 \mu\text{M}$   $^{55}\text{Fe}$  ferric citrate [1:20; Fe(III)] or  $1 \mu\text{M}$   $^{55}\text{Fe}$  ferrous ascorbate [1:50; Fe(II)]. At 15 min (arrow), a 10-fold excess ( $10 \mu\text{M}$ ) of cold iron (in the same chemical form) was added (closed symbols) or not (open symbols). Accumulation of  $^{55}\text{Fe}$  by the cells was followed. Values shown are means  $\pm$  SD from four experiments.

of excess cold iron simultaneously with that of  $^{55}\text{Fe}$ . In all cases, we observed a simple effect of isotopic dilution (data not shown). Thus, presumably, a few minutes after addition of  $^{55}\text{Fe}$ , a significant proportion of this iron was not in solution but was bound to the surface of the cells, preventing isotopic dilution by excess cold iron. As the experimental procedure included washing with strong ferrous and ferric chelators before counting  $^{55}\text{Fe}$  associated with the cells (see "Materials and Methods"), these putative binding sites appear to have high affinity. Two different effects of adding excess cold iron at 15 min on uptake of  $^{55}\text{Fe}$  were observed according to the algae species, to the redox state of iron, and to the growth conditions. In some cases, the amount of  $^{55}\text{Fe}$  associated with the cells continued to increase after the addition of cold iron (Figs. 6 and 7). This is consistent with the  $^{55}\text{Fe}$  binding to high-affinity binding sites at the cell surface prior to internalization during the chase and with surface iron being removed by the iron chelators during the washing step. In other conditions (depending on the species and on the amount of iron in the growth medium), addition of cold iron resulted in a decrease of  $^{55}\text{Fe}$  associated with the cells (Figs. 6 and 7). This was evident, for example, for ferrous iron uptake by diatoms grown in Mf medium containing  $0.1 \mu\text{M}$  iron (Fig. 6) or for ferric iron uptake by *O. tauri* and *E. huxleyi* grown in low-iron ( $2 \text{ nM}$ ) Mf medium (Fig. 7). This effect is more difficult to interpret. Possibly,  $^{55}\text{Fe}$  bound to the cell surface was not removed by the iron chelators during the washing step but could be displaced by excess cold iron, leading to a net decrease of  $^{55}\text{Fe}$  associated with the cells after

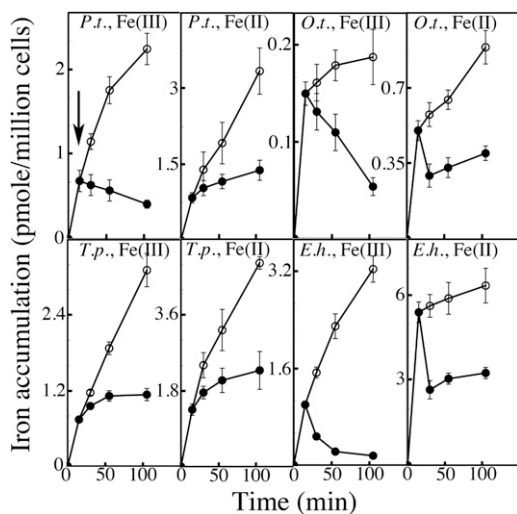


**Figure 7.** Pulse-chase uptake of iron (2). *P. tricornutum* (*P.t.*), *O. tauri* (*O.t.*), *T. pseudonana* (*T.p.*), and *E. huxleyi* (*E.h.*) cells grown for 1 week in low-iron Mf medium (2 nM iron) were incubated in uptake buffer with either 1  $\mu\text{M}$   $^{55}\text{Fe}$  ferric citrate [1:20; Fe(III)] or 1  $\mu\text{M}$   $^{55}\text{Fe}$  ferrous ascorbate [1:50; Fe(II)]. At 15 min (arrow), a 100-fold excess (100  $\mu\text{M}$ ) of cold iron (in the same chemical form) was added (closed symbols) or not (open symbols). Accumulation of  $^{55}\text{Fe}$  by the cells was followed. Values shown are means  $\pm$  SD from three experiments.

cold iron addition. Alternatively, iron may be exported from the cells to the medium: net uptake would result from equilibrium between iron influx and efflux. This possibility was not investigated further.

These pulse-chase experiments indicate that iron uptake by marine microalgae is not a simple process in which iron in the bulk solution directly accesses the uptake sites. It is likely that there is an iron-binding step at the cell surface prior to uptake, as suggested previously (Hudson and Morel, 1990; Sutak et al., 2010). This binding step differed between algae species and varied according to the cell iron status. For example, the patterns of pulse-chase uptake of ferrous iron by *P. tricornutum* differed between cells grown in high-iron and in low-iron media (Figs. 6 and 7), suggesting that the ability of cells to bind iron at the cell surface depends on the cell iron status.

### Iron Bound to the Cell Surface Is Poorly Exchangeable by Iron Chelators

Cells of the various species were incubated at 0°C for 5 min with 1  $\mu\text{M}$   $^{55}\text{Fe}$ (III)-citrate or  $^{55}\text{Fe}$ (II)-ascorbate and then washed with various iron chelators. All five species specifically bound large amounts of both ferric and ferrous iron; the proportion of this bound iron displaced by strong iron chelators depended on the species (Supplemental Fig. S3). For example, most of the iron bound to *E. huxleyi* within 5 min remained bound after repeated washing with strong iron chelators (Supplemental Fig. S3); however, in pulse-chase experiments, about 50% (ferrous iron) to more than 90% (ferric iron) of the  $^{55}\text{Fe}$  bound to *E. huxleyi* cells was

removed by cold iron chasing (Fig. 7). This experiment suggests that the rapid phase of iron uptake observed especially for ferrous iron following a shift to high-iron medium (see day 1 in Fig. 2) involved high-affinity iron binding at the cell surface.

We followed the percentage of iron that remained in solution in a growth medium containing 0.1  $\mu\text{M}$   $^{55}\text{Fe}$ (III)-citrate (Fig. 8). Most of the iron rapidly became associated with the cells, and for some species (namely both diatom species), only a few percent of the iron remained in solution after 24 h. This confirms that the cells bind and concentrate iron at the cell surface.

### Proteins Involved in Iron Uptake/Binding

Next, we investigated whether some of the iron associated with cells during iron uptake kinetics was bound to proteins and/or accumulated into protein(s). Cells were grown under standard conditions and then incubated for 1 and 3 h with  $^{55}\text{Fe}$ (III)-citrate or  $^{55}\text{Fe}$ (II)-ascorbate. Total protein extracts were prepared and subjected to native gel electrophoresis. The gels were dried and autoradiography was used to identify iron-containing bands (Fig. 9 for *P. tricornutum*, *O. tauri*, and *E. huxleyi*). In *P. tricornutum*, some of the iron from both ferric citrate and ferrous ascorbate accumulated, with the same efficiency, in a protein (or a protein

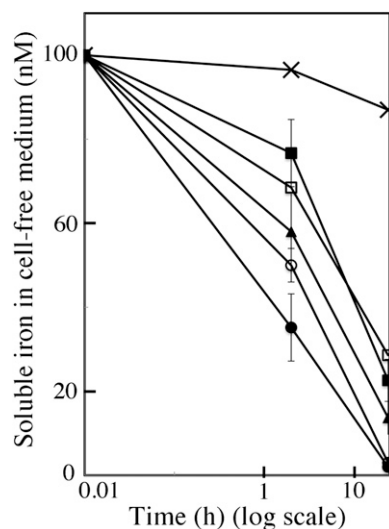


**Figure 8.** Evolution of soluble iron in the growth medium. Mf medium containing 100 nM  $^{55}\text{Fe}$ (III)-citrate (1:20) was left free of cells (crosses) or was inoculated at time 0 with 5 million cells  $\text{mL}^{-1}$  (open circles, *P. tricornutum*; closed circles, *T. pseudonana*; triangles, *E. huxleyi*) or 50 million cells  $\text{mL}^{-1}$  (open squares, *O. tauri*; closed squares, *M. pusilla*). Before inoculation, cells were precultured for 1 week in Mf medium containing 0.1  $\mu\text{M}$  iron, harvested, washed once with uptake buffer containing 1 mM BPS, 1 mM DFOB, and 50 mM EDTA, and then washed twice with iron-free Mf medium. Aliquots of the media were taken at 2 and 24 h, centrifuged for 20 min at 10,000g, and the supernatant was assayed for iron. Values shown are means  $\pm$  SD from three experiments.



complex) of high molecular mass (although the ferrireductase of cells was not induced). Similarly, in *O. tauri*, some of the iron accumulated in a high-molecular-mass protein, but to a greater extent from ferrous ascorbate than ferric citrate. In *E. huxleyi*, most of the iron bound to proteins was associated with high-molecular-mass complexes (greater than 1,000 kD), and possibly photosystems and respiratory chain complexes, although two faint bands were visible, one between the 242- and 480-kD markers and another around the 66-kD marker. None of these bands increased in intensity between 1 and 3 h of incubation of the cells with iron, inconsistent with the corresponding proteins being iron storage proteins. The amount of iron associated with *E. huxleyi* proteins did not differ according to whether the iron source was ferric or ferrous iron, although there was a very faint additional band when ferric iron was the iron source (Fig. 9). The main *P. tricornutum* and *O. tauri* bands associated with iron were excised from the gels, and the proteins contained were analyzed by mass spectrometry (MS; Supplemental Table S2). Separation of proteins by native gel electrophoresis allows much less resolution than separation by SDS-PAGE; therefore, we identified numerous proteins from the excised bands (Supplemental Table S2). Among these, we looked for proteins putatively involved in iron metabolism. The *O. tauri* proteins loaded with iron included ferritin (band around 480 kD in Fig. 9; Mascot score of 60.4). The major *P. tricornutum* band loaded with iron (between 242 and 480 kD in Fig. 9) did not contain ferritin or any other protein with known iron-binding properties, but it did contain Isip1 (for iron starvation-induced protein; with a high Mascot score of 181.6). *ISIP1* is induced by iron starvation in *P. tricornutum* (Allen et al., 2008) and other marine microalgae (Marchetti et al., 2012), but its role remains unknown. Our results suggest that this protein could play a role in iron uptake by *P. tricornutum*. However,

these results are still preliminary: further purification steps will be required to identify unambiguously ferritin and Isip1 as the main proteins loaded with iron during iron uptake kinetics in *O. tauri* and *P. tricornutum*, respectively (and to identify iron-binding proteins in other species). This work is in progress in our laboratories.

Although these experiments do not allow one to determine which part of total iron associated with the cells was bound to proteins, our findings are consistent (qualitatively) with the iron uptake kinetics for whole cells (compare Figs. 4 and 9): *P. tricornutum* can take up iron from ferric and from ferrous iron sources even when the ferrireductase activity of the cells is not induced; *O. tauri* preferentially uses ferrous iron, despite no clear evidence of ferrireductase activity in this species; *E. huxleyi*, which has no reductase activity, can use both ferric and ferrous iron with comparable efficiency. This correspondence between enzymological and biochemical data is consistent with the notion that iron binding cannot be dissociated from iron uptake per se in a large panel of marine microalgae: iron binding to the cell surface is probably part of the uptake process itself, regardless of the ability of cells to reduce iron or not.

## DISCUSSION

Interest in the iron uptake mechanisms used by marine phytoplankton is increasing due to the importance of phytoplankton in the carbon cycle and in primary oxygen production. The number of species for which the genome is sequenced is also increasing, facilitating the analysis of the molecular basis of iron uptake (for review, see Morrissey and Bowler, 2012; Shaked and Lis, 2012). Here, we report investigations into iron uptake from different iron sources by marine microalgae species belonging to different phyla and from different ecological niches. We aimed to establish experimentally whether different strategies are used preferentially by different species to acquire iron from the medium and to determine the conditions, if any, in which iron uptake mechanisms are induced/repressed. The main strategies of iron uptake by unicellular eukaryotes include reductive and nonreductive uptake of iron (see introduction). Both strategies are used in yeast (Lesuisse and Labbe, 1989) and have been well characterized. The nonreductive strategy of iron uptake generally involves the use of siderophores but may also involve the direct uptake of aqueous ferric ions (Sutak et al., 2010), although no such mechanism has been described at the molecular level. However, it is unclear whether the known mechanisms are relevant to the marine environment. Iron levels in surface seawater are generally extremely low (0.02–1 nM; Turner et al., 2001), and no mechanism of iron uptake (reductive or nonreductive) with affinity constants in the nanomolar range has ever been described. The marine environment also has other characteristics, relevant to uptake, including, in particular, the high diffusion rate

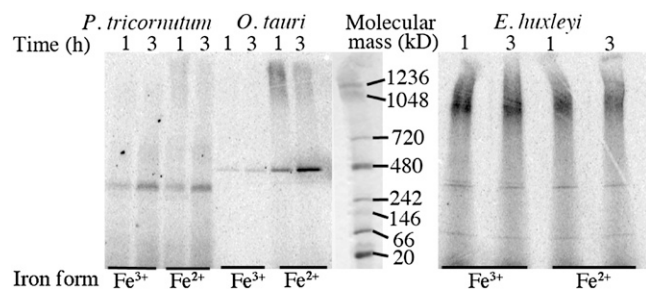


**Figure 9.** Autoradiography of dried gels after separation of whole-cell extracts on blue native PAGE. *P. tricornutum*, *O. tauri*, and *E. huxleyi* cells were incubated in uptake buffer with either 1  $\mu\text{M}$   $^{55}\text{Fe}$  ferric citrate ( $\text{Fe}^{3+}$ ) or 1  $\mu\text{M}$   $^{55}\text{Fe}$  ferrous ascorbate ( $\text{Fe}^{2+}$ ) for 1 and 3 h as indicated. Cells were washed twice with Mf medium by centrifugation, and whole-cell extracts were prepared as described in “Materials and Methods.” After native PAGE (about 25  $\mu\text{g}$  of protein per lane), the gels were dried and autoradiographed. Major iron-containing bands in *P. tricornutum* and *O. tauri* extracts were excised from the gel and analyzed by MS.

of the relevant species (siderophores or reduced iron; Völker and Wolf-Gladrow, 1999).

Genes homologous to those encoding yeast/plant ferrireductases (*FRE/FRO* family), the yeast multicopper ferroxidase (*FET*), and the yeast/plant ferrous ions transporters (*NRAMP*, *ZIP* family) have been identified in several marine microalgae (Armbrust et al., 2004; Allen et al., 2008; for review, see Morrissey and Bowler, 2012). However, there is a lack of experimental data concerning how these components may contribute to the very efficient iron uptake mechanisms required by marine microalgae.

Ferrous iron was taken up more rapidly than ferric iron by all the species we studied, suggestive of reductive iron uptake. However, direct measurement identified cell ferrireductase activities only for the diatoms *P. tricornutum* and *T. pseudonana*. In *P. tricornutum*, this activity was induced only under strict iron starvation conditions, as expected from transcriptomic analyses (Allen et al., 2008). By contrast, ferrireductase appeared to be constitutive and highly active (comparable to the activity of iron-deprived yeast cells) in *T. pseudonana*, and this was not predicted by transcriptomic analyses (Kustka et al., 2007). The ferrireductase activity of both diatoms was inhibited by DPI, a powerful inhibitor of the yeast ferrireductase (Lesuisse et al., 1996) and of the human neutrophil NADPH oxidase (Doussi re and Vignais, 1992), which suggests that these proteins of the Fre family are conserved flavohemoproteins. We found no clear evidence of ferrireductase activity in the other three species, although the green algae *O. tauri* and *M. pusilla* were able to transfer electrons to the non-permeant dye resazurin, and this activity was not inhibited by DPI. Therefore, the transplasma membrane electron transfer in these species does not appear to be catalyzed by a member of the Fre family. The coccolithophore *E. huxleyi* showed no transplasma membrane electron transfer activity at all, like the alveolate *C. velia* (Sutak et al., 2010). All the species we studied were thus able to use  $\text{Fe}^{2+}$  as an iron source, regardless of the presence and/or induction of a ferrireductase system.

Systems for ferrous uptake in the species that are unable to reduce iron may serve to acquire iron naturally reduced by photoreduction (Sunda, 2001; Sunda and Huntsman, 2003). All the species we studied were also able to use ferric iron, although ferrous iron was clearly the preferred iron source in some species (e.g. *O. tauri*). Experimental evidence and comparative genomics studies led several authors to propose the yeast reductive iron uptake system as a paradigm for iron uptake by some diatoms (Allen et al., 2008; Morrissey and Bowler, 2012) or even more generally for the eukaryotic phytoplankton (Shaked et al., 2005). However, in yeast, iron reduction is a prerequisite for iron uptake, such that the flux of iron entering the cells from a ferric complex is directly dependent on the cell ferrireductase activity (except for siderophores, for which yeast cells have specific receptors) and does not depend on the stability constants of the ferric complex (Lesuisse et al., 1987). In addition, iron uptake in yeast

by the high-affinity mechanism is controlled kinetically, via the channeling of iron through the Fet3/Ftr1 complex (Kwok et al., 2006), meaning that the rate of iron uptake does not decrease when the concentration of ferric ligands increases. This is not what we observed in marine microalgae, even in diatoms expressing inducible or constitutive ferrireductase activity. Consistent with previous reports (Hudson and Morel, 1990; Sunda, 2001), the rate of iron uptake from any ferric iron source (citrate, EDTA, desferrichrome, DFOB) by the species we studied decreased sharply with increasing ligand-Fe (III) ratio. This is not what is observed in yeast but similar to *C. velia* (Sutak et al., 2010). This suggests that iron uptake is dissociative:  $\text{Fe}^{3+}$  ions bound to the putative permease or to surface binding sites equilibrate with the bulk phase. In this model (called the "Fe' model"), the rate of iron uptake is controlled thermodynamically and is limited by the concentration of unchelated iron (Fe') in the medium (Morel et al., 2008).

The situation is thus complicated: our data and previous findings (Morel et al., 2008) indicate that the limiting step for iron uptake is controlled thermodynamically, depending on the concentration of unchelated iron (Fe'). However, this raises an "insoluble" biological problem: the solubility of iron is very low, so how do cells acquire an ionic species (Fe') in solution at concentrations ranging from  $10^{-16}$  to  $10^{-19}$  M? Reduction greatly increases the solubility of iron and, thus, the concentration of iron available to the cells (Shaked et al., 2005; Shaked and Lis, 2012). Thus, even if we did not observe, in any of the species we studied, that iron reduction was a prerequisite for uptake, the presence of a ferrireductase system is expected to increase the amount of aqueous iron available to the cells. However, the ability of some species to reduce iron does not solve the problem of iron acquisition in a very-low-iron environment: if the ferrous species generated were in equilibrium with the bulk solution, reduction would not help cells in an environment where iron is present in nanomolar concentrations, unless iron reduction would be tightly coupled to a ferrous iron uptake system controlled kinetically and with a  $K_d$  ( $K_a$ ) in the nanomolar range.

Experiments comparing the well-characterized iron uptake systems of yeast with iron uptake systems in marine microalgae can help resolve this issue. Yeast cells take up iron directly from the bulk solution, as shown by pulse-chase experiments. In contrast, analogous experiments show that in all the microalgae we studied, iron uptake involved an additional step of binding at the cell surface. Addition of cold iron during  $^{55}\text{Fe}$  uptake never resulted in simple isotopic dilution, indicating that iron uptake is preceded by binding to the cell surface. Iron bound to the cells was not readily displaced by strong iron chelators, as observed previously in *P. carterae* (Hudson and Morel, 1990), indicating that it was specific and high affinity. This is in apparent contradiction with the observation that an increase in the ligand-to-iron ratio resulted in a large decrease in iron uptake; however, this observation only shows that

iron equilibrates with the bulk phase at some stage of the uptake process. One possibility, which we propose as a general model (Fig. 10), is that binding of iron from the medium at the cell surface would be controlled thermodynamically, and in a further step this bound iron would escape simple thermodynamics rules, being no more in equilibrium with the bulk solution. This would account for this striking paradox: (1) in all the species we studied, iron associated with the cells decreased dramatically with increasing the concentration of ligand and the stability constant of ferric complexes; and (2) iron bound to the cells was not readily displaced by strong iron chelators.

Different mechanisms could account for the strong binding of iron at the cell surface. In *T. pseudonana*, there is an interconnection between the genes regulated by iron and by silicon, and it has been suggested that iron could be incorporated with silicon into the cell wall (Mock et al., 2008; Morrissey and Bowler, 2012). Iron may also bind to specific iron-binding proteins at the surface, as in the complex mechanism described in *Dunaliella salina*, where two transferrin-like proteins form a complex with a multicopper ferroxidase and a glycoprotein at the surface to take up iron (Paz et al., 2007). Whatever the mechanism involved, accumulation of iron at the surface of the cells as such would not facilitate uptake if this iron were still in equilibrium with the bulk solution, as we noted previously (Sutak et al., 2010). Iron binding at the cell surface might be controlled thermodynamically and iron-binding components might specifically interact with uptake proteins (possibly homologous to proteins found in yeast and higher plants, like Fet3, Fetrl, Nramp, or Irt-like proteins, or alternatively completely

undescribed proteins), involving a cooperative, kinetically controlled process. Further work is required to identify the molecular components involved in the binding and uptake of iron by the different species. We started to do so by a proteomic approach, which allows one to propose that ferritin and Isip1 are involved in iron uptake/storage in *O. tauri* and *P. tricornutum*, respectively. This is a fruitful approach that we are currently developing in our laboratories.

The critical surface binding step may explain the apparent paradox we observed concerning the induction/repression of uptake as a function of the growth conditions: iron uptake rates appeared higher for the first few days following a shift to high-iron medium than to low-iron medium. Induction of iron uptake occurred only after several days in iron-deficient medium. But the pattern of kinetics also changed between the first stage (early induction in high-iron medium) and the second stage (later induction in iron-deficient medium): in the first stage of induction under high-iron conditions, the iron uptake rate increased most during the first 30 to 60 min after iron addition, and then uptake slowed down; in the second stage of induction under iron limitation, less iron associated with the cells within the first 30 to 60 min after iron addition, but iron uptake progressed continuously over the following 2 h (Fig. 4). This might reflect a change in the iron-binding capacity of the cells between the two situations. Excess iron may result in specific binding of iron at the surface, whereas iron limitation may induce iron incorporation into the cells. This effect of an increased capacity of iron binding induced by iron addition is similar to findings for *E. huxleyi* (Boye and van den Berg, 2000). As pointed out by the authors, this increase in the capacity of cells to

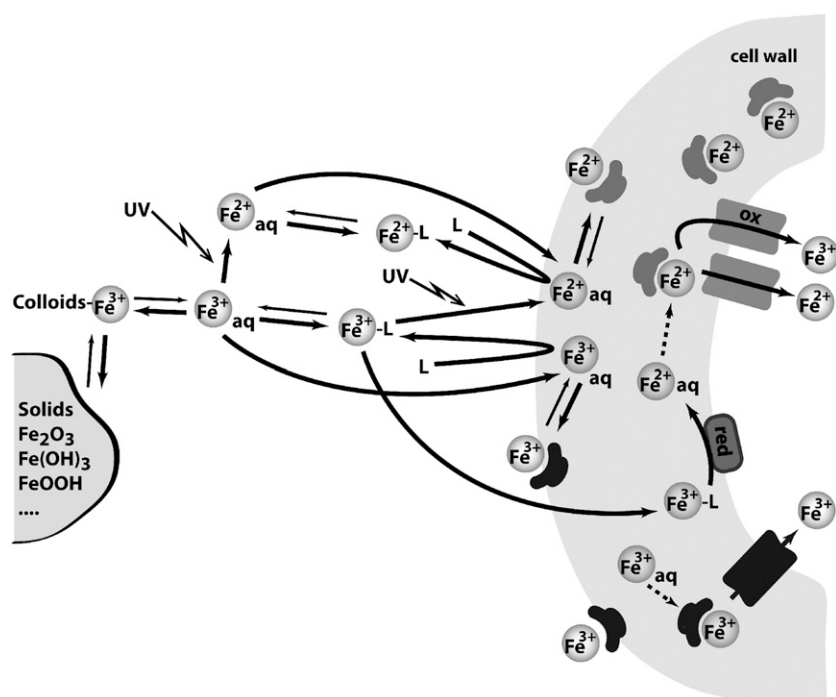


**Figure 10.** Tentative model of iron uptake by marine microalgae. Several different iron species interact in the ocean (solid iron, colloid iron, liganded [L] iron, or aqueous ferric and ferrous species), some of which are theoretically accessible for transport by the phytoplankton. Aqueous  $\text{Fe}^{3+}$  and  $\text{Fe}^{2+}$  (generated either by photoreduction or via the cell ferrireductase activity) bind to the cell wall of the cells (black and gray symbols, respectively), resulting in a higher local concentration of this element near the transport sites. This iron equilibrates with the bulk phase in a first stage (binding sites oriented toward the exterior) but becomes poorly exchangeable with ferric and ferrous chelators in a second stage (binding sites oriented toward the interior). Uptake of iron per se occurs via unknown interactions between binding sites and transport sites, which can involve proteins homologous to that described in yeast and plants (Fet, Nramp, Irt-like proteins, etc.) and/or uncharacterized proteins.

bind iron induced by iron itself is contrary to the concept of siderophores, which are normally synthesized when iron is limiting (Boye and van den Berg, 2000). Possibly, marine microalgae have developed an adaptation allowing large quantities of iron to be bound when the iron concentration increases transiently in their environment, which can be used subsequently during periods of iron scarcity.

In conclusion, this work strengthens two main hypotheses. Our first hypothesis is that iron uptake in marine microalgae can only be understood if a cell surface binding step is considered. We are currently trying to identify iron-binding components at the surface of various microalgae. Our second hypothesis is that most microalgae can take up both ferric and ferrous iron, regardless of the presence/absence of a ferrereductase system, and therefore that nonreductive uptake of iron as described previously for *C. velia* (Sutak et al., 2010) is probably common in marine microalgae.

## MATERIALS AND METHODS

### Strains, Cell Culture, and Media

The yeast *Saccharomyces cerevisiae* YPH499 was grown at 30°C in iron-rich (yeast nitrogen base) or iron-deficient (yeast nitrogen base + 0.1 mM BPS) medium as described previously (Lesuisse et al., 2001). Microalgae were grown at 20°C under a 16/8-h light (3,000 lux)/dark regime in a filtered Mf medium as described previously (Sutak et al., 2010). The composition of Mf medium (standard medium used for cell growth) was as follows (for 1 L of medium): sea salts (Sigma) 40 g (composition: Cl<sup>-</sup> 19.29 g, Na<sup>+</sup> 10.78 g, SO<sub>4</sub><sup>2-</sup> 2.66 g, Mg<sup>2+</sup> 1.32 g, K<sup>+</sup> 420 mg, Ca<sup>2+</sup> 400 mg, CO<sub>3</sub><sup>2-</sup>/HCO<sub>3</sub><sup>-</sup> 200 mg, Sr<sup>2+</sup> 8.8 mg, BO<sub>2</sub><sup>-</sup> 5.6 mg, Br<sup>-</sup> 56 mg, I<sup>-</sup> 0.24 mg, Li<sup>+</sup> 0.3 mg, F<sup>-</sup> 1 mg); MOPS 250 mg (pH 7.3); NH<sub>4</sub>NO<sub>3</sub> 2.66 mg; NaNO<sub>3</sub> 75 mg; Na<sub>2</sub>SiO<sub>3</sub>·0.5H<sub>2</sub>O 22.8 mg; NaH<sub>2</sub>PO<sub>4</sub> 15 mg; 1 mL of vitamin stock (thiamine-HCl 20 mg L<sup>-1</sup>, biotin 1 mg L<sup>-1</sup>, B12 1 mg L<sup>-1</sup>); 1 mL of trace metal stock (MnCl<sub>2</sub>·0.4H<sub>2</sub>O 200 mg L<sup>-1</sup>, ZnSO<sub>4</sub>·0.7H<sub>2</sub>O 40 mg L<sup>-1</sup>, Na<sub>2</sub>MoO<sub>4</sub>·0.2H<sub>2</sub>O 20 mg L<sup>-1</sup>, CoCl<sub>2</sub>·0.6H<sub>2</sub>O 14 mg L<sup>-1</sup>, Na<sub>3</sub>VO<sub>4</sub>·nH<sub>2</sub>O 10 mg L<sup>-1</sup>, NiCl<sub>2</sub> 10 mg L<sup>-1</sup>, H<sub>2</sub>SeO<sub>3</sub> 10 mg L<sup>-1</sup>); and 1 mL of antibiotic stock (ampicillin sodium and streptomycin sulfate 100 mg mL<sup>-1</sup>). Iron was added in the form of ferric citrate (1:20). Under standard conditions of growth (for routine maintenance of the cultures), iron concentration was 0.1 μM.

The composition of uptake medium (buffer used to measure iron uptake kinetics) was as follows: 480 mM NaCl, 20 mM KCl, 0.1 mM MgCl<sub>2</sub>, 0.1 mM CaCl<sub>2</sub>, and 10 mM MOPS (pH 7.3). Uptake medium was used instead of Mf medium to measure iron uptake in order to minimize the interactions of iron ligands with Ca<sup>2+</sup> and Mg<sup>2+</sup> ions (the concentrations of which are 10 and 54 mM, respectively, in the Mf medium). The chemical speciation of iron was estimated using GEOCHEM-EZ software (<http://www.plantmineralnutrition.net/Geochem/geochem%20home.htm>; Shaff et al., 2010). The algae species used were obtained from the Roscoff culture collection (<http://www.sb-roscoff.fr/Phyto/RCC/index.php>): *Phaeodactylum tricornutum* RCC69, *Thalassiosira pseudonana* RCC950, *Ostreococcus tauri* RCC745, *Micromonas pusilla* RCC827, and *Emiliania huxleyi* RCC1242. To analyze the responses of cells to a sudden decrease or increase in the iron concentration in the medium, we proceeded as follows. Cells from standard cultures (0.1 μM iron as ferric citrate) were harvested and washed twice with iron-free Mf medium. They were resuspended in Mf medium containing either 0.01 μM iron (low-iron condition) or 1 μM iron (high-iron condition) and grown for 1 week. The cells were harvested by centrifugation and washed once with a buffer containing 480 mM NaCl, 20 mM KCl, 0.1 mM MgCl<sub>2</sub>, 0.1 mM CaCl<sub>2</sub>, 1 mM BPS, 1 mM DFOB, 50 mM EDTA, and 10 mM MOPS (pH 7.3) and twice with iron-free Mf medium to remove traces of iron chelators. Aliquots were resuspended in 500 mL of high-iron medium (2 μM iron) and 500 mL of iron-deficient medium (no iron added). Cells were harvested from samples of 50 to 100 mL collected every day, washed with strong iron chelators as described above, and used for uptake and ferrereductase assays. When the cultures reached the end of the exponential growth phase, they were diluted to 500 mL with the same iron-rich or iron-deficient medium.

### Iron Uptake Assays

Iron uptake by yeast was assayed on microtiter plates as described previously (Lesuisse et al., 2001). Iron uptake by microalgae was assayed on microtiter plates under shaking in the light or in the dark at 20°C. Iron uptake assays were performed with concentrated cell suspensions (50–250 million cells per 100 μL) incubated in the uptake medium described above. <sup>55</sup>Fe (29,600 MBq mg<sup>-1</sup>) was added to the appropriate concentration in the form of ferrous ascorbate, ferric citrate, ferric EDTA, ferrioxamine B, or ferrichrome. Iron uptake was stopped after various periods by adding 0.1 mM BPS, 0.1 mM DFOB, and 5 mM EDTA (final concentrations) to the cell suspensions and incubating for 2 min. The cells were then collected with a cell harvester (Brandel), washed three times on the filter with the uptake buffer containing 10 mM EDTA and 1 mM salicyl hydroxamic acid, and counted in a Wallac 1450 Micro Beta Trilux scintillation counter. To avoid quenching, cell pigments were bleached with sodium hypochlorite before scintillation counting. Determination of iron storage and binding under various conditions was also performed by using <sup>55</sup>Fe (29,600 MBq mg<sup>-1</sup>).

### Reductase Assays

Whole-cell ferrereductase activity expressed by microalgae was measured as described previously (Lesuisse and Labbe, 1989) with Fe(III)-EDTA (0.5 mM) as the iron source. The cells (50–500 million cells per mL) were incubated in Mf medium at 20°C in the presence of iron (0.5 mM) and ferrozin (1.5 mM) for various times and then centrifuged at 10,000g for 10 min. The absorbency (562 nm) of the supernatant was then measured ( $\epsilon = 25.7 \text{ mm}^{-1} \text{ cm}^{-1}$ ). Transplasma membrane electron transfer was assessed for whole cells with resazurin as the electron acceptor. Reductase activity was recorded as the appearance of resorufin at 30°C with a Jobin Yvon JY3D spectrofluorimeter ( $\lambda_{\text{ex}} = 560 \text{ nm}$ ,  $\lambda_{\text{em}} = 585 \text{ nm}$ , slit widths of 2 nm for both excitation and emission). The incubation mixture was 50 mM sodium citrate buffer (pH 6.5; yeast) or Mf medium (algae) containing 10 mM resazurin and was stirred magnetically.

### Electrophoresis

Cells were disrupted by sonication, and proteins were solubilized with 0.5% digitonin. Samples were analyzed by blue native PAGE using the Novex Native PAGE Bis-Tris Gel System (3%–12%) according to the manufacturer's (Invitrogen) protocol. The gels were vacuum dried and autoradiographed.

### MS Analysis

Gel plugs were rehydrated with 20 μL of 25 mmol L<sup>-1</sup> NH<sub>4</sub>HCO<sub>3</sub> containing sequencing-grade trypsin (12.5 μg mL<sup>-1</sup>; Promega) and incubated overnight at 37°C. The resulting peptides were sequentially extracted with 30% acetonitrile, 0.1% trifluoroacetic acid and 70% acetonitrile, 0.1% trifluoroacetic acid. Digests were analyzed with a LTQ Velos Orbitrap (Thermo Fisher Scientific) coupled to an Easy nano-LC Proxeon system (Thermo Fisher Scientific). Peptides were separated chromatographically on a Proxeon C18 Easy Column (10 cm, 75 μm i.d., 120 Å), at 300 nL min<sup>-1</sup> flow, with a gradient rising from 95% solvent A (water-0.1% formic acid) to 25% B (100% acetonitrile, 0.1% formic acid) in 20 min, then to 45% B in 40 min, and finally to 80% B in 10 min. The peptides were analyzed in the Orbitrap in full ion scan mode at a resolution of 30,000, a mass range of 400 to 1,800 mass-to-charge ratio, and with a MS full scan maximum ion time of 100 ms. Fragments were obtained with collision-induced dissociation activation with a collisional energy of 35%, an activation collisional endothermicity of 0.250 for 10 ms, and analyzed in the LTQ in a second scan event. The ion-trap MS/MS maximum ion time was 50 ms. MS/MS data were acquired in a data-dependent mode in which the 20 most intense precursor ions were isolated, with a dynamic exclusion of 20 s and an exclusion mass width of 10 ppm. Data were processed with Proteome Discoverer 1.3 software (Thermo Fisher Scientific) coupled to an in-house Mascot search server (Matrix Science; version 2.3.02). The mass tolerance of fragment ions was set to 10 ppm for precursor ions and 0.6 D for fragments. The following modifications were used in variable parameters: oxidation (Met) and phosphorylations (Ser/Thr/Tyr). The maximum number of missed cleavages was limited to two for trypsin digestion. MS/MS data were compared with the *Ostreococcus* and *Phaeodactylum* sequence databases extracted from the National Center for Biotechnology Information nonredundant database. A reversed database approach was used for the false discovery rate estimation. A threshold of 5% was chosen for this rate.

Sequence data from this article can be found in the GenBank/EMBL data libraries under accession numbers listed in Supplemental Table S2.

## Supplemental Data

The following materials are available in the online version of this article.

**Supplemental Figure S1.** Reductase activity of *O. tauri*, *M. pusilla*, and *E. huxleyi* with resazurin as the electron acceptor.

**Supplemental Figure S2.** Iron uptake recorded in the dark and in the light.

**Supplemental Figure S3.** Iron binding by the microalgae cells at 0°C.

**Supplemental Table S1.** Effect of iron concentration on growth rate and cell yield.

**Supplemental Table S2.** Mass spectrometry results corresponding to Figure 9.

## ACKNOWLEDGMENTS

We thank Régis Chambert for fruitful discussions and for his help with interpreting data.

Received July 23, 2012; accepted September 28, 2012; published October 2, 2012.

## LITERATURE CITED

- Allen AE, Laroche J, Maheswari U, Lommer M, Schauer N, Lopez PJ, Finazzi G, Fernie AR, Bowler C (2008) Whole-cell response of the pennate diatom *Phaeodactylum tricornutum* to iron starvation. *Proc Natl Acad Sci USA* **105**: 10438–10443
- Allen MD, del Campo JA, Kropat J, Merchant SS (2007) FEA1, FEA2, and FRE1, encoding two homologous secreted proteins and a candidate ferrireductase, are expressed coordinately with FOX1 and FTR1 in iron-deficient *Chlamydomonas reinhardtii*. *Eukaryot Cell* **6**: 1841–1852
- Anderson MA, Morel FMM (1982) The influence of aqueous iron chemistry on the uptake of iron by the coastal diatom *Thalassiosira weissflogii*. *Limnol Oceanogr* **27**: 789–813
- Armbrust EV, Berges JA, Bowler C, Green BR, Martinez D, Putnam NH, Zhou S, Allen AE, Apt KE, Bechner M, et al (2004) The genome of the diatom *Thalassiosira pseudonana*: ecology, evolution, and metabolism. *Science* **306**: 79–86
- Blaiseau P-L, Seguin A, Camadro JM, Lesuisse E (2010) Iron uptake in yeasts. In P Cornelis, SC Andrews, eds, *Iron Uptake and Homeostasis in Microorganisms*. Caister Academic Press, Brussels, pp 265–284
- Bowler C, Allen AE, Badger JH, Grimwood J, Jabbari K, Kuo A, Maheswari U, Martens C, Maumus F, Otilar RP, et al (2008) The *Phaeodactylum* genome reveals the evolutionary history of diatom genomes. *Nature* **456**: 239–244
- Boye M, van den Berg CMG (2000) Iron availability and the release of iron-complexing ligands by *Emiliania huxleyi*. *Mar Chem* **70**: 277–287
- Butler A (1998) Acquisition and utilization of transition metal ions by marine organisms. *Science* **281**: 207–210
- Butler A (2005) Marine siderophores and microbial iron mobilization. *Biometals* **18**: 369–374
- Cepicka I, Elias M, Hampl V (2010) Řád z Chaosu. *Vesmír* **89**: 464–469
- Doussière J, Vignais PV (1992) Diphenylene iodonium as an inhibitor of the NADPH oxidase complex of bovine neutrophils: factors controlling the inhibitory potency of diphenylene iodonium in a cell-free system of oxidase activation. *Eur J Biochem* **208**: 61–71
- Finazzi G, Moreau H, Bowler C (2010) Genomic insights into photosynthesis in eukaryotic phytoplankton. *Trends Plant Sci* **15**: 565–572
- Hopkinson BM, Morel FM (2009) The role of siderophores in iron acquisition by photosynthetic marine microorganisms. *Biometals* **22**: 659–669
- Hudson RJM, Morel FMM (1990) Iron transport in marine phytoplankton: kinetics of cellular and medium coordination reactions. *Limnol Oceanogr* **35**: 1002–1020
- Kosman DJ (2003) Molecular mechanisms of iron uptake in fungi. *Mol Microbiol* **47**: 1185–1197
- Kustka AB, Allen AE, Morel FMM (2007) Sequence analysis and transcriptional regulation of iron acquisition genes in two marine diatoms. *J Phycol* **43**: 715–729
- Kwok EY, Severance S, Kosman DJ (2006) Evidence for iron channeling in the Fet3p-Ftr1p high-affinity iron uptake complex in the yeast plasma membrane. *Biochemistry* **45**: 6317–6327
- Lesuisse E, Blaiseau PL, Dancis A, Camadro JM (2001) Siderophore uptake and use by the yeast *Saccharomyces cerevisiae*. *Microbiology* **147**: 289–298
- Lesuisse E, Casteras-Simon M, Labbe P (1996) Evidence for the *Saccharomyces cerevisiae* ferrireductase system being a multicomponent electron transport chain. *J Biol Chem* **271**: 13578–13583
- Lesuisse E, Labbe P (1989) Reductive and non-reductive mechanisms of iron assimilation by the yeast *Saccharomyces cerevisiae*. *J Gen Microbiol* **135**: 257–263
- Lesuisse E, Raguzzi F, Crichton RR (1987) Iron uptake by the yeast *Saccharomyces cerevisiae*: involvement of a reduction step. *J Gen Microbiol* **133**: 3229–3236
- Maldonado MT, Allen AE, Chong JS, Lin K, Leus D, Karpenko N, Harris SL (2006) Copper-dependent iron transport in coastal and oceanic diatoms. *Limnol Oceanogr* **51**: 1729–1743
- Marchetti A, Parker MS, Moccia LP, Lin EO, Arrieta AL, Ribalet F, Murphy ME, Maldonado MT, Armbrust EV (2009) Ferritin is used for iron storage in bloom-forming marine pennate diatoms. *Nature* **457**: 467–470
- Marchetti A, Schrueth DM, Durkin CA, Parker MS, Kodner RB, Berthiaume CT, Morales R, Allen AE, Armbrust EV (2012) Comparative metatranscriptomics identifies molecular bases for the physiological responses of phytoplankton to varying iron availability. *Proc Natl Acad Sci USA* **109**: E317–E325
- Mawji E, Gledhill M, Milton JA, Tarran GA, Ussher S, Thompson A, Wolff GA, Worsfold PJ, Achterberg EP (2008) Hydroxamate siderophores: occurrence and importance in the Atlantic Ocean. *Environ Sci Technol* **42**: 8675–8680
- Merchant SS, Allen MD, Kropat J, Moseley JL, Long JC, Tottey S, Terauchi AM (2006) Between a rock and a hard place: trace element nutrition in *Chlamydomonas*. *Biochim Biophys Acta* **1763**: 578–594
- Mock T, Samanta MP, Iverson V, Berthiaume C, Robison M, Holtermann K, Durkin C, Bondurant SS, Richmond K, Rodesch M, et al (2008) Whole-genome expression profiling of the marine diatom *Thalassiosira pseudonana* identifies genes involved in silicon bioprocesses. *Proc Natl Acad Sci USA* **105**: 1579–1584
- Monnier A, Liverani S, Bouvet R, Jesson B, Smith JQ, Mosser J, Corellou F, Bouget FY (2010) Orchestrated transcription of biological processes in the marine picoeukaryote *Ostreococcus* exposed to light/dark cycles. *BMC Genomics* **11**: 192
- Morel FMM, Kustka AB, Shaked Y (2008) The role of unchelated Fe in the iron nutrition of phytoplankton. *Limnol Oceanogr* **53**: 400–404
- Morrissey J, Bowler C (2012) Iron utilization in marine cyanobacteria and eukaryotic algae. *Front Microbiol* **3**: 43
- Naito K, Imai I, Nakahara H (2008) Complexation of iron by microbial siderophores and effects of iron chelates on the growth of marine microalgae causing red tides. *Phycol Res* **56**: 58–67
- Not F, Latasa M, Marie D, Cariou T, Vaultou D, Simon N (2004) A single species, *Micromonas pusilla* (Prasinophyceae), dominates the eukaryotic picoplankton in the Western English Channel. *Appl Environ Microbiol* **70**: 4064–4072
- Paz Y, Katz A, Pick U (2007) A multicopper ferroxidase involved in iron binding to transferrins in *Dunaliella salina* plasma membranes. *J Biol Chem* **282**: 8658–8666
- Philpott CC (2006) Iron uptake in fungi: a system for every source. *Biochim Biophys Acta* **1763**: 636–645
- Philpott CC, Protchenko O (2008) Response to iron deprivation in *Saccharomyces cerevisiae*. *Eukaryot Cell* **7**: 20–27
- Rue EL, Bruland KW (1995) Complexation of iron(III) by natural organic ligands in the Central North Pacific as determined by a new competitive ligand equilibration/adsorptive cathodic stripping voltammetric method. *Mar Chem* **50**: 117–138
- Seguin A, Sutak R, Bulteau AL, Garcia-Serres R, Oddou JL, Lefevre S, Santos R, Dancis A, Camadro JM, Latour JM, et al (2010) Evidence that yeast frataxin is not an iron storage protein in vivo. *Biochim Biophys Acta* **1802**: 531–538
- Shaff JE, Schultz BA, Craft EJ, Clark RT, Kochian LV (2010) GEOCHEM-EZ: a chemical speciation program with greater power and flexibility. *Plant Soil* **330**: 207–214
- Shaked Y, Kustka AB, Morel FMM (2005) A general kinetic model for iron acquisition by eukaryotic phytoplankton. *Limnol Oceanogr* **50**: 872–882

- Shaked Y, Lis H** (2012) Disassembling iron availability to phytoplankton. *Front Microbiol* **3**: 123
- Silva AMN, Le Kong X, Parkin MC, Cammack R, Hider RC** (2009) Iron(III) citrate speciation in aqueous solution. *Dalton Trans* **40**: 8616–8625
- Soria-Dengg S, Horstmann U** (1995) Ferrioxamines B and E as iron sources for the marine diatom *Phaeodactylum tricornutum*. *Mar Ecol Prog Ser* **127**: 269–277
- Sunda W, Huntsman S** (2003) Effect of pH, light, and temperature on Fe-EDTA chelation and Fe hydrolysis in seawater. *Mar Chem* **84**: 35–47
- Sunda WG** (2001) Bioavailability and bioaccumulation of iron in the sea. *In* DR Turner, KA Hunter, eds, *The Biogeochemistry of Iron in Seawater*. John Wiley & Sons, Chichester, UK, pp 41–84
- Sutak R, Slapeta J, San Roman M, Camadro JM, Lesuisse E** (2010) Non-reductive iron uptake mechanism in the marine alveolate *Chromera velia*. *Plant Physiol* **154**: 991–1000
- Turner DR, Hunter KA, de Baar HJW** (2001) Introduction. *In* DR Turner, KA Hunter, eds, *The Biogeochemistry of Iron in Seawater*. John Wiley & Sons, Chichester, UK, pp 1–7
- Völker C, Wolf-Gladrow DA** (1999) Physical limits on iron uptake mediated by siderophores or surface reductases. *Mar Chem* **65**: 227–244
- Vukosav P, Mlakar M** (2010) Iron(III)-organic complexes dissolved in seawater: characterization of iron(III)-succinate and iron(III)-malate complexes in aqueous solution. *Rapp Comm Int Mer Médit* **39**: 321
- Wu J, Boyle E, Sunda W, Wen LS** (2001) Soluble and colloidal iron in the oligotrophic North Atlantic and North Pacific. *Science* **293**: 847–849